
The ELM Neuron: an Efficient and Expressive Cortical Neuron Model Can Solve Long-Horizon Tasks.

Aaron Spieler^{1,2}, Nasim Rahaman^{3,2}, Georg Martius^{1,2}, Bernhard Schölkopf², and Anna Levina^{1,4}

¹University of Tübingen

²Max Planck Institute for Intelligent Systems, Tübingen

³Mila, Quebec AI Institute

⁴Max Planck Institute for Biological Cybernetics, Tübingen

Abstract

Traditional large-scale neuroscience models and machine learning utilize simplified models of individual neurons, relying on collective activity and properly adjusted connections to perform complex computations. However, each biological cortical neuron is inherently a sophisticated computational device, as corroborated in a recent study where it took a deep artificial neural network with millions of parameters to replicate the input-output relationship of a detailed biophysical model of a cortical pyramidal neuron. We question the necessity for these many parameters and introduce the Expressive Leaky Memory (ELM) neuron, a biologically inspired, computationally expressive, yet efficient model of a cortical neuron. Remarkably, our ELM neuron requires only 8K trainable parameters to match the aforementioned input-output relationship accurately. We find that an accurate model necessitates multiple memory-like hidden states and intricate nonlinear synaptic integration. To assess the computational ramifications of this design, we evaluate the ELM neuron on various tasks with demanding temporal structures, including a sequential version of the CIFAR-10 classification task, the challenging Pathfinder-X task, and a new dataset based on the Spiking Heidelberg Digits dataset. Our ELM neuron outperforms most transformer-based models on the Pathfinder-X task with 77% accuracy, demonstrates competitive performance on Sequential CIFAR-10, and superior performance compared to classic LSTM models on the variant of the Spiking Heidelberg Digits dataset. These findings indicate a potential for biologically motivated, computationally efficient neuronal models to enhance performance in challenging machine learning tasks.

1 Introduction

The human brain has impressive computational capabilities, yet the precise mechanisms underpinning them remain largely undetermined. Two complementary directions are pursued in search of mechanisms for brain computations. On the one hand, many researchers investigate how these capabilities could arise from the collective activity of neurons connected into a complex network structure [50, 18, 22], where individual neurons might be as basic as leaky integrators or ReLU neurons. On the other hand, it has been proposed that the intrinsic computational power possessed by individual neurons [39, 40, 59] contributes a significant part to the computations.

Even though most work focuses on the former hypothesis, an increasing amount of evidence indicates that cortical neurons are remarkably sophisticated [59, 1, 20, 47], even comparable to expressive multilayered artificial neural networks [58, 32, 66, 65, 5, 53, 35, 36, 57], and capable of discriminating between dozens to hundreds of input patterns [58, 24, 25, 54]. Numerous biological

mechanisms, such as complex ion channel dynamics (e.g. NMDA nonlinearity [52, 46, 63]), plasticity on various and especially longer timescales (e.g. slow spike frequency adaptation [38, 4]), the intricate cell morphology (e.g. nonlinear integration by dendritic tree [61, 57, 47]), and their interactions, have been identified to contribute to their complexity.

Thus, one of the central questions in computational neuroscience is which learning and memory capabilities can be attributed to an individual cortical neuron and how mechanisms within a single neuron can work together to generate the observed computational complexity.

Detailed biophysical models of cortical neurons aim to capture this inherent complexity through high-fidelity simulations [26, 27, 1]. However, they require a lot of computing resources to run and typically operate at a very fine level of granularity that does not facilitate the extraction of higher-level insights into the neuron’s computational principles. A promising approach to deriving such higher-level insights from simulations is through the training of surrogate phenomenological neuron models. These models are designed to replicate the output of high-fidelity biophysical simulations but use simplified interpretable components. This approach was employed, for example, to model computation in the dendritic tree via simple two-layer ANN [58, 65, 66]. Building on this line of research, a recent study by Beniaguev et al. [5] developed a temporal convolutional network to capture the spike-level input/output (I/O) relationship with millisecond precision, accounting for the complexity of integrating diverse synaptic input across the entirety of the dendritic tree of a high-fidelity biophysical neuron model. It was found that a highly expressive temporal convolutional network with millions of parameters was essential to reproduce the aforementioned I/O relationship.

In this work, we propose that a model equipped with appropriate inductive biases that align with the operational principles of a cortical neuron should be capable of capturing the I/O relationship using a substantially smaller model size. To achieve this, a model would likely need to integrate multiple mechanisms of neural expressivity and judiciously allocate computational resources and parameters in close analogy to biological neurons. Should such a construction be possible, the requisite design choices may yield insights into higher-level principles of neural computation. We proceed to design the Expressive Leaky Memory (ELM) neuron model (see Figure 1), a biologically inspired, computationally expressive, yet parameter-efficient phenomenological model of a cortical neuron. The ELM neuron functions as a recurrent cell and can be conveniently used as a drop-in replacement for LSTMs [28].

Our experiments show that a variant of the ELM neuron is expressive enough to accurately match the spike level I/O of a detailed biophysical model of a layer 5 pyramidal neuron at a millisecond temporal resolution with merely 8K parameters, in stark contrast to the millions of parameters required by temporal convolutional networks. To understand the implications of this design, we first probe the ELM neuron for its temporal information integration capabilities on a challenging biologically-inspired dataset requiring the addition of spike-encoded spoken digits. We find that the ELM neuron can outperform classic LSTMs, highlighting ELM neuron’s ability to leverage long-term memory. We subsequently evaluate the ELM neuron on three well-established long sequence modeling tasks prevalent in the machine learning literature, including the notoriously challenging Pathfinder-X task where it achieves 77.3% accuracy even though many transformer-based models struggle to learn at all.

Our contributions are the following.

1. We propose the Expressive Leaky Memory (ELM) neuron model, a recurrent architecture that combines expressiveness with computational and parameter efficiency. The design of the ELM neuron is inspired by the structure and functionality of a biological cortical neuron.
2. Our experiments reveal that the ELM neuron effectively expresses the input/output relationship of a sophisticated biophysical model of a cortical neuron, suggesting that the inductive biases we introduced into the ELM neuron align with the operating principles of biological neurons.
3. We further demonstrate the ELM neuron’s ability to integrate temporal information over extended time horizons. Additionally, we show its capacity to handle complex long-range sequence modeling tasks that are common in machine learning, affirming its potential applicability in broader machine learning contexts.

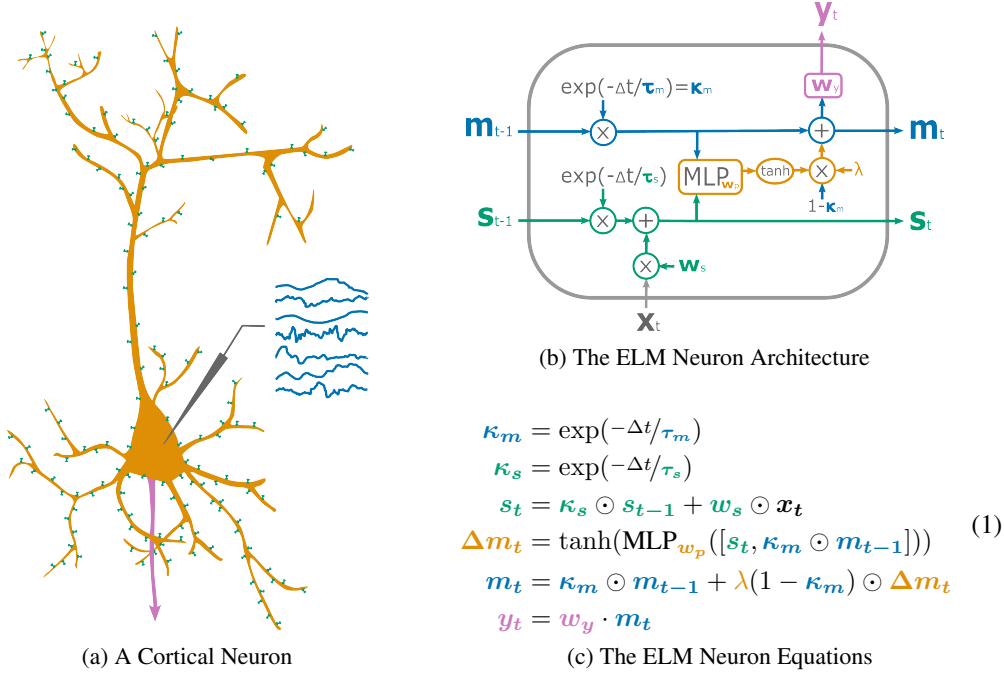


Figure 1: **The biologically motivated Expressive Leaky Memory (ELM) neuron model.** The architecture can be divided into the following components; the input **current synapse dynamics**, the **integration mechanism dynamics**, the **leaky memory dynamics**, and the **output dynamics**. **a)** Sketch of a biological cortical pyramidal neuron segmented into the analogous architectural components using the corresponding colors. **b)** Schematics of the ELM neuron architecture, component-wise colored accordingly. **c)** The ELM neuron equations, where $x_t \in \mathbb{R}^{d_s}$ is the input at time t , $\Delta t \in \mathbb{R}^+$ the fictitious elapsed time in milliseconds between two consecutive inputs x_{t-1} and x_t , $m \in \mathbb{R}^{d_m}$ are memory units, $s \in \mathbb{R}^{d_s}$ the synapse currents (traces), $\tau_m \in \mathbb{R}^{+d_m}$ and $\tau_s \in \mathbb{R}^{+d_s}$ their respective timescales in milliseconds, $w_s \in \mathbb{R}^{+d_s}$ are synapse weights, w_p the weights of a *Multilayer Perceptron* (MLP) with l_{mlp} hidden layers of size d_{mlp} , $w_y \in \mathbb{R}^{d_o \times d_m}$ the output weights, $\lambda \in \mathbb{R}^+$ a scaling factor for the delta memory $\Delta m_t \in \mathbb{R}^{d_m}$, and $y \in \mathbb{R}^{d_o}$ the output.

2 The Expressive Leaky Memory Neuron

In this section, we discuss the design of the Expressive Leaky Memory (ELM) neuron, biologically motivating the individual computational components and the overall recurrent cell architecture.

2.1 Architectural Components

The current synapse dynamics. Neurons typically receive inputs at their synapses in the form of sparse binary events, known as spikes, which are generally converted into small positive or negative currents exhibiting characteristic temporal dynamics [37]. A prevalent abstraction in computational neuroscience for this dynamic is the current-based synapse model [15, 8], which we also adopt in the Expressive Leaky Memory (ELM) neuron model (refer to the **green** components in Figure 1). In essence, s_t represents a low-pass filtered version of potentially sparse binary input, rendering it beneficial for coincidence detection or synaptic information integration [41]. The synapse weights, w_s , function as a straightforward gating mechanism, serving to either amplify or attenuate the input.

The memory unit dynamics. The state of a biological neuron can be characterized by diverse measurable quantities, such as the membrane voltage, various ion or protein concentrations (e.g. Ca⁺, synaptic vesicles, ATP, etc.), and their slow or fast decay (determined by their respective timescale constants). Each of these quantities carries information through time, acting as a sort of memory mechanism or hidden state [37, 15] (see **blue** components in figure 1). Most computational neuroscience models *a priori* fix which quantities to track (usually the membrane voltage or certain ion

concentrations and their interactions) and the relationships between them (through differential equations). However, which of these biological quantities are computationally relevant, how they interact, how many integration zones a neuron has, and what the relevant timescales of these processes remain topics of active debate [2, 27, 1, 39, 11]. Therefore, to match a biological neuron’s computations and expressivity accurately, the surrogate model architecture needs to accommodate a large range of possibilities. In the ELM neuron, we achieve this by making the number of memory units d_m a hyperparameter, unlike most other computational neuroscience models. Additionally, motivated by the large diversity of timescales found within and across neurons [10], and their computational importance [21, 16, 71], the memory units m_t are equipped with individually learnable memory timescales τ_m , defining their respective rate of decay (large timescales meaning slower decay), constituting a learnable yet constant forgetting mechanism.

The integration mechanism dynamics. This dynamic refers to how dependent on the previous memory units m_{t-1} the synaptic input s_t is integrated into the memory unit updates Δm_t in analogy to the dendritic tree of cortical neuron (orange components in Figure 1). We choose to parameterize this transformation using a Multilayer Perceptron (MLP), which is motivated by the ongoing discussion regarding the complexity and functional form of synaptic information integration over the dendritic tree in cortical neurons. While earlier perspectives suggested an integration process akin to linear summation [34], newer studies advocate for complex non-linear integration [1, 20, 47], specifically proposing multi-layered ANNs as a more suitable model [58, 32, 65, 53, 35, 36, 29], making an MLP a natural choice. Furthermore, its ability to incorporate previous memory units m_{t-1} into the process accommodates state-dependent synaptic integration and related computations [30, 17, 6], and enables the relationships between memory units m to be fully learnable, irrespective of their quantity. These features provide our neuron model with enhanced flexibility over those using pre-determined differential equations.

The output dynamics. Spiking neurons emit their output spike at the axon hillock when the membrane voltage crosses an (approximate and varying) threshold [37]. For the ELM neuron, we chose a flexible linear readout layer w_y on top of the memory units (none of which have to correspond to membrane voltage *a priori*). The output of the readout layer can be a real value between 0 and 1, representing an output spike probability (in neuroscience attributed as a momentary rate), which ensures higher compatibility with typical machine learning tasks. Therefore, similar to biophysical models (e.g. Hodgkin Huxley [30]), there is no explicit reset mechanism, refractoriness, post-spike dynamics. All of these are implicitly learned by the ELM neuron. To instantiate an ELM neuron as a spiking neural network, a simple output rectification could be applied to recover binary output [70].

Additional design choices. We found that enabling greater changes Δm_t by introducing a multiplicative factor λ (a hyperparameter) improved training performance. Furthermore, note that the factor κ_m is parametrized with $\exp(-\Delta t/\tau_m)$ (derived from classic neuron models [15]) and we learn the timescales τ_m directly (constrained using a *sigmoid* to the the desired range). As opposed to learning κ_m and initializing it with $1 - \Delta t/\tau_m$, we get valid decay constants even for $\tau_m < \Delta t$, and observed improved training stability.

3 Related Work

Accurately replicating the full spike-level input/output (I/O) relationship of detailed biophysical neuron models at millisecond resolution in a computationally efficient manner presents a formidable challenge. However, addressing this task could potentially yield valuable insights into neural mechanisms of expressivity, learning, and memory capabilities.

The relative scarcity of prior work on this subject can be partially attributed to the computational complexity of cortical neurons only recently garnering increased attention [65, 5, 47, 57]. Additionally, traditional phenomenological neuron models have primarily aimed to replicate specific computational phenomena of neurons or networks [39, 31, 27], rather than the entire I/O relationship. Finally, the computational resources and tooling necessary for an extensive exploration of suitable designs have only recently become widely available.

Phenomenological modeling research on temporally or spatially less detailed I/O relationship of biophysical neurons has been primarily centered around the use of multi-layered ANN structures in

analogy to the neurons dendritic tree [58, 65, 66]. Similarly, we parametrize the synaptic integration with an **MLP**, while crucially extending this modeling perspective in several ways. Drawing upon the principles of classical phenomenological modeling via differential equations [31, 15], our approach embraces the recurrent nature inherent to neurons. We further consider the significance of hidden states m beyond membrane voltage, as seen in prior works with predetermined variables [7, 19]. This addition enables us to flexibly investigate internal memory timescales τ_m , hinted at in earlier modeling studies [21, 10].

The relationship between timescales and the computations in the brain is the topic of numerous recent investigations in neuroscience. It was shown that intrinsic timescales are diverse across the cortex [56], which can lead to increased neural expressivity [21, 10]. A common way they occur in computational neuroscience is through the variables capturing slowly building up or leaking out biophysical quantities [30, 55, 15]. While timescales can be shaped by task requirements [16, 71, 13], longer neuronal timescales might be used for temporal credit assignment across larger time horizons [3].

Deep learning architectures explicitly incorporating timescales have recently become more prevalent, with several recent architectures based on RNN, transformers or state-space models successfully incorporating them for improved temporal information processing [23, 51, 60, 49]. Initially, they appeared in Leaky-RNN [55, 33, 43, 62], which use a convex combination of old memory and update (as done in ELM using κ_m). In contrast to a time-varying memory decay or complex multi-staged gating architectures, the ELM features a much simpler recurrent cell architecture only using fixed but trainable time constants τ_m and a single **MLP** to parametrize its integration dynamics.

Comparison with common RNN structures like LSTM [28] and GRU [12] surface two major differences. First, we set κ_m as a trainable constant instead of using parametric input and forget gating mechanisms [62]. Second, we utilize an **MLP** instead of a simpler parametric affine transformation for calculating Δm_t . Therefore, in contrast with most previous research, our architecture puts the primary importance not on the various gates, also leaving the forget gate constant during inference (which is otherwise believed to be hugely important [67]), but rather on the memory update vector calculation itself.

4 Experiments

In the experimental section of this work, we address three primary research questions. **First**, are the inductive biases imparted in the ELM neuron adequate to accurately fit a high-fidelity biophysical simulation with a small number of parameters? We detail this investigation in Section 4.1. **Second**, is the ELM neuron capable of effectively integrating temporal information? We explore this issue in Section 4.2. **Third**, we test whether the ELM neuron is expressive enough to solve tasks with complex and long-range dependencies, which is discussed in Section 4.3. Each of these questions contributes to our overall understanding of the ELM neuron’s capabilities and its potential applications in both biological and machine learning contexts.

4.1 Fitting a complex biophysical cortical neuron model’s input-output relationship

The NeuronIO dataset primarily consists of simulated input-output (I/O) data for a complex biophysical layer 5 cortical pyramidal neuron model [26]. Input data features biologically inspired spiking patterns (1278 pre-synaptic spike channels), while output data comprises the model’s somatic membrane voltage and output spikes (see Figure 2a and 2b). The dataset and related code is publicly available [5]. The dataset was pre-processed in accordance with [5], and the models were trained using Binary Cross Entropy (BCE) for spike prediction and Mean Squared Error (MSE) for somatic voltage prediction, with equal weighting.

Our **ELM** neuron achieves better prediction of voltage and spikes than previously used architectures for any given number of trainable parameters (and compute). In particular, it crosses the “sufficiently good” spike prediction performance threshold (0.991 AUC) as defined in [5] by using merely 50K trainable parameters, which is around $200\times$ improvement compared to the previous attempt (**TCN**) that required around 10M trainable parameters, and $6\times$ improvement over a **LSTM** baseline which requires around 266K parameters (see Figure 2c-d). Overall, this result indicates that recurrent computation is indeed an appropriate inductive bias for modeling cortical neurons.

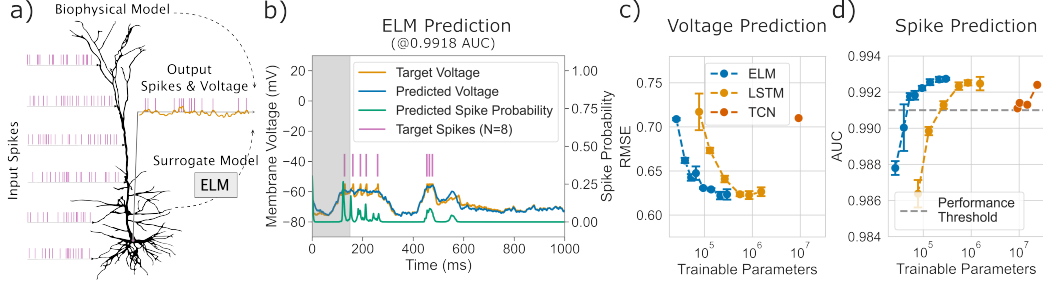


Figure 2: The ELM neuron is a computationally efficient model of cortical neuron. **a)** detailed biophysical model of a layer 5 cortical pyramidal cell was used to generate the NeuronIO dataset consisting of input spikes and output spikes and voltage. **b)** Example target and predictions by the first **ELM** neuron that crosses the performance threshold. **c) and d)** Voltage and spike prediction performance of the respective surrogate models. While previous works required around 10M parameters to make accurate spike predictions using a **TCN** [5], an **LSTM** baseline is able to do it with 266K, and our **ELM** neuron model requires merely 53K, simultaneously achieving much better voltage prediction performance than the **TCN**. Additional figures comparing FLOPS in appendix.

We use the fitted model to investigate how many memory units and which timescales are needed to match the neuron closely. We find that around 20 memory units are required (Figure 3a) with timescales that are allowed to reach at least 25 ms (Figure 3d). While a diversity of timescales including long ones seem to be favorable for accurate modeling (Figure 3d and 3f), using constant

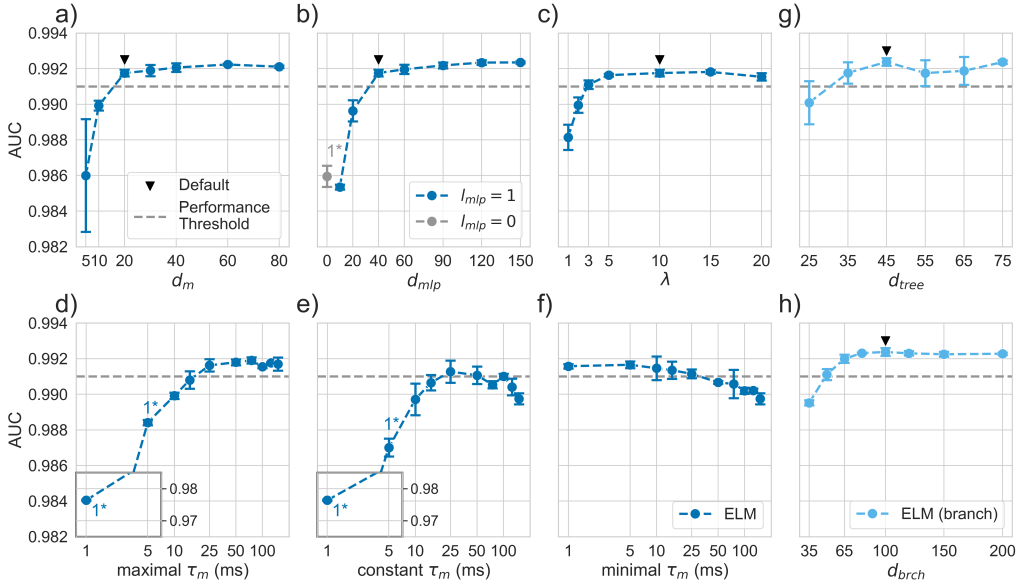


Figure 3: The ELM neuron gives relevant neuroscientific insights. Ablations on NeuronIO of different hyperparameters of an **ELM** neuron with $AUC \approx 0.992$, and a (**branch**) **ELM** with the same default hyperparameters. Number of removed divergent runs marked with 1*. **a)** We find between 10 and 20 memory-like hidden states to be required for accurate predictions, much more than typical phenomenological models use [31, 15]. **b)** Highly nonlinear integration of synaptic input is required, in line with recent neuroscientific findings [61, 36, 47]. **c)** Allowing greater updates to the memory units is beneficial. **d-f)** Ablations of memory timescale (initialization and bounding) range or (constant) value, with default range being 1ms-150ms. Timescales around 25 ms seem to be the most useful (matching the typical membrane timescale in the cortex [15]); however, a lack can be partially compensated by longer timescales. **g) and h)** Ablating the number of branches d_{tree} and number of synapses per branch d_{brch} of the (**branch**) **ELM** neuron.

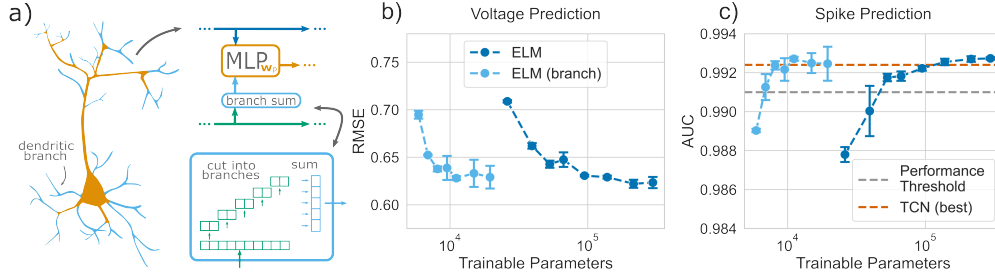


Figure 4: **Coarse-grained modeling of synaptic integration significantly improves model efficiency.** **a)** The **integration mechanism dynamics** of the ELM now computes the activity of individual dendritic branches as a simple sum of their respective synaptic inputs first before passing them on to the MLP_{w_p} , where d_{tree} is the number of branches and d_{brch} the number of synapses per branch. **b-c)** Produced using joint ablation of d_m with $d_{mlp} = 2d_m$. The new (**branch**) ELM neuron further improves on the vanilla ELM neuron by about $7\times$ in terms of parameter efficacy. A (**branch**) ELM model with a humble 8104 trainable parameters now reaches 0.9924 AUC (3rd from left), using otherwise same hyper-parameters as the ELM (6th from right).

memory timescales around 25 ms performs surprisingly well (matching the typical membrane timescales used in computational modeling [15], Figure 3e). Removing the hidden layer or decreasing the integration mechanism complexity deteriorates the performance significantly (Figure 3b). Allowing for more rapid changes of the memory through larger λ is necessary (Figure 3c), possibly to match the fast internal dynamics of neurons around spike times.

How much nonlinearity is in the dendritic tree? Within the ELM architecture, we allow for nonlinear interaction between any two synaptic inputs via the MLP. This flexibility might be necessary in cases where little is *a priori* known about the structure of the input. However, for matching the I/O of biological neurons, knowledge of neuronal morphology and biophysical assumptions about *linear-nonlinear* computations in the dendritic tree might be exploited to reduce the dimensionality of the input to the MLP, which so far is particularly costly due to the large number of synaptic inputs it receives ($d_s = 1278$). In particular, many studies suggest individual dendritic branches compute a rectified sum of their synaptic inputs [58, 61, 25, 57], with additional nonlinearities located downstream. Consequently, we modify the ELM neuron to include virtual branches along which the synaptic input is first reduced by a simple summation before further processing (see Figure 4). For NeuronIO specifically, we assign the synaptic inputs to the branches in a moving window fashion (exploiting that in the dataset, neighboring inputs were also typically neighboring synaptic contacts on the same dendritic branch of the biophysical model). The window size is controlled by the branch size, and number of branches implicitly defines the stride size to ensure equally spaced sampling across the $d_s = 1278$ inputs.

Surprisingly, even with this strong simplification, the (**branch**) ELM neuron model is able to retain its predictive performance while requiring a modest 8K trainable parameters to substantially cross the performance threshold. This corresponds to roughly $7\times$ reduction over the vanilla ELM neuron. We also find that a combination of $d_{tree} = 35$ and $d_{brch} = 65$ still achieved over 0.991 AUC with only 5479 trainable parameters, corroborating the assumption of the near-linear computation within dendritic branches and inviting future investigation of minimal required synaptic nonlinearity. However, this simplification ideally utilizes the knowledge of the exact morphology for modeling the neuron, or the relationship structure in the input data in case of other tasks; thus most consecutive experimental reports are for the vanilla ELM neuron.

4.2 Evaluating temporal information integration capabilities on a bio-inspired task

The Spiking Heidelberg Digits (SHD) dataset comprises spike-encoded spoken digits (0-9) in German and English [14]. The digits were encoded using 700 input channels in a biologically-inspired artificial cochlea. Each channel represents a narrow frequency band with the firing rate coding for the signal power in this band, resulting in an encoding that resembles the spectrogram of the spoken digit (see Figure 5a).

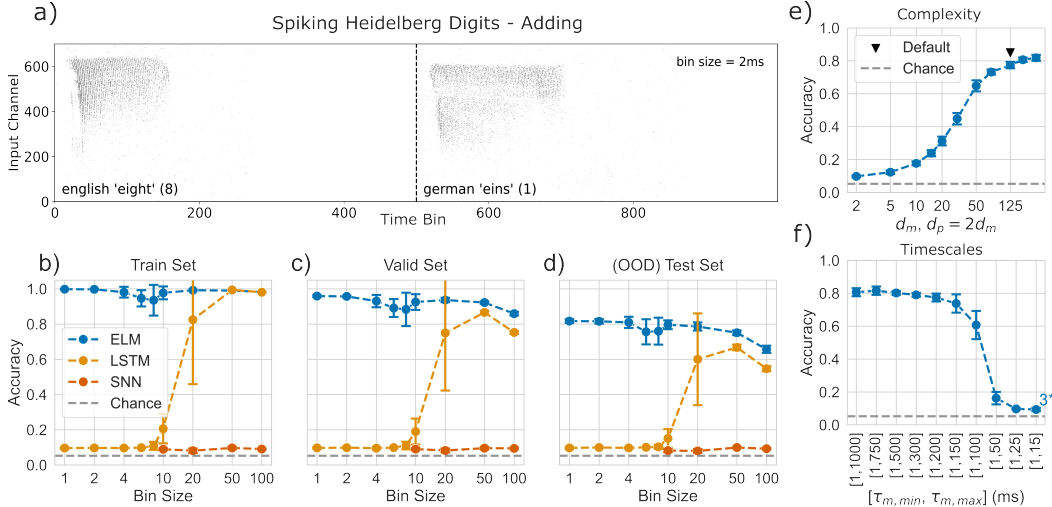


Figure 5: The ELM neuron performs well on long and sparse data using longer timescales. a) Sample from the biologically motivated SHD-Adding dataset (based on [14]), each dot is an input spike, and a vertical dashed line is a guide for the eye indicating the separation of the two digits (not communicated to the network). **b-d)** The ELM neuron consistently outperforms a classic LSTM, especially for smaller bin sizes (meaning longer training samples), and LSTM-performance cannot be fully recovered even for larger bin sizes. Our Leaky Integrate and Fire (LIF) Spiking Neural Network (SNN) does not manage to achieve good performance for any bin size, and training becomes unstable for long sequences. **e) and f)** Ablations using bin size of 2ms with test set performance reported. **e)** Solving SHD-Adding requires ELM neuron to have a higher complexity than required for NeuronIO. **f)** Longer memory timescales are crucial for extracting long-range dependencies in the data.

Motivated by recent findings that most neuromorphic benchmark datasets only require very limited temporal processing abilities [69], we introduce the SHD-Adding dataset, created by concatenating two uniformly and independently sampled SHD digits and setting the target to their sum (regardless of language) (see Figure 5a). Solving this dataset necessitates identifying each digit on a shorter timescale and computing their sum by integrating this information over a longer timescale, which in turn requires retaining the first digit in memory. Whether single cortical neurons can solve this exact task is unclear; however, it has been shown that even single neurons possibly encode and perform basic arithmetics in the medial temporal lobe [9, 44, 45].

The ELM neuron demonstrates its ability to solve the summing task across various temporal resolutions, as determined by the bin size. As we vary the bin size from 1ms (comprising 2000 bins in total, corresponding to the maximum temporal detail and longest required memory retention) to 100 (with 20 bins in total, corresponding to the minimum temporal detail and shortest memory retention), the ELM neuron’s performance remains robust, degrading only gracefully for greater bin sizes (see Figure 5b-d). Further, the performance is also maintained when testing on two held-out speakers, showing that the ELM neuron remains comparatively robust out-of-distribution. In contrast, the LSTM struggles with this task, especially when the bin size is below 50, due to memory issues. As the bin size increases, the LSTM’s performance does not improve because larger bin sizes leads to the loss of crucial temporal details. This outcome underlines the importance of a model’s ability to integrate complex synaptic information effectively (see Figure 5e). It also highlights the need for models to accommodate longer memory timescales, in light of the observation that limiting our model to memory timescales below 150 has a severe impact on performance (see Figure 5f).

4.3 Evaluating on complex and very long temporal dependency tasks

To test the extent of the ELM neuron’s ability to extract complex long-range dependencies, we use three modern machine learning tasks. The Sequential CIFAR-10 task involves solving the 10-way CIFAR-10 [42] classification problem given a flattened sequence of 1024 pixel values, corresponding to 32×32 sized images [64]. The Pathfinder and Pathfinder-X tasks [48, 64] require determining whether two dots are connected by a path in a 2D image (see Figure 6, but the images are flattened

Table 1: Long Sequence Modeling Datasets

Model	Accuracy		
	Sequential CIFAR-10	Pathfinder	Pathfinder-X
ELM Neuron (ours)	54.0	74.72	77.3
Chrono-LSTM [62]	46.61	70.79	51.85
Transformer [68]	42.44	71.4	FAIL
Longformer [3]	42.22	69.71	FAIL
S4 [23]	87.26	86.05	88.1
Mega [49]	90.44	96.01	97.98

The ELM neuron can solve long-range sequence modeling tasks. Results on three complex temporal dependency tasks. Surprisingly, the simple ELM architecture is able to solve the notoriously challenging Pathfinder-X task with sample length $> 16K$. It scores higher than the transformer baselines and is only outperformed by big 6-staged architectures tuned specifically for these tasks (S4, Mega).

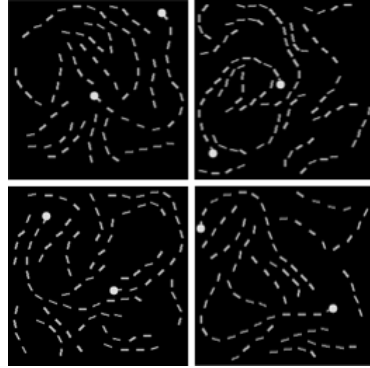


Figure 6: **Pathfinder-X Samples.** The task is to classify whether two dots are connected by a dashed line. Each 128×128 image is flattened to a sequence in raster-scan order, yielding sequences of total length 16384.

out to be a sequence of pixels before being fed into the model. For the Pathfinder-X task, the length of this sequence is 16384, corresponding to a 128×128 image (see Figure 6), making it a notoriously difficult long-range modeling task.

Our results are summarized in Table 1, where we compare the ELM neuron against several strong baselines. The model most comparable to ours is an LSTM with explicit long timescale-derived gating bias initialization [62] (Chrono-LSTM). We also incorporate two self-attention-based models, including the Transformer [68] and the Longformer [3]. Finally, we include Structured State Space Sequence model [23] (S4) and a Transformer leveraging exponential moving averages [49] (Mega), the latter being the current state-of-the-art.

When comparing between recurrent cells (ELM Neuron vs. Chrono-LSTM), we find that both models solve the tasks, albeit the ELM Neuron substantially outperforms Chrono-LSTM on the Pathfinder-X task. The self-attention-based models trail further behind, with both Transformer and Longformer failing to solve the Pathfinder-X task [64]. S4 and Mega perform better, but they are both deep architectures; Mega features 6 layers of 128 and 256 memory cells and self-attention, compared to the ELM neuron with 150 memory units and less than 100K parameters.

Overall, the results suggest that the ELM neuron is capable of solving tasks with very long temporal dependencies and doing so without employing multistage structures. We hypothesize that assembling the ELM neurons into layered network structures might give it enough processing capabilities to catch up with the deep models but leave this investigation to future work.

5 Conclusion

In this study, we introduced a biologically inspired recurrent cell, the Expressive Leaky Memory (ELM) neuron, and demonstrated its capability to fit the full spike-level input/output mapping of a high-fidelity biophysical neuron model. Unlike previous works that achieved this fit with millions of parameters, our a variant of our model only requires eight thousand, thanks to the careful design of the architecture leveraging appropriate implicit biases. Furthermore, the ELM neuron can effectively model a cortical neuron without making rigid assumptions about the number of memory states, unlike existing phenomenological models. It also imposes fewer presumptions about the complexity of the integration mechanism and the exact values of the timescales associated with each memory state.

We further scrutinized the implications of this design on various tasks, including some notoriously challenging ones in the machine learning literature. The ELM neuron was found to be competitive, a notable feat considering its biological motivation, a characteristic often lacking in similar successful models. However, we acknowledge the ongoing debate regarding the degree of "biological plausibility" required in intelligent systems. Biological systems, including neurons, are subject to a variety of 'wetware' constraints that may not need to be reproduced.

Despite this caveat, the promising performance of the ELM neuron on machine learning tasks suggests that we are beginning to incorporate the inductive biases that drive the development of more intelligent systems. Future research focused on connecting ELM neurons into a network could provide even more insights into the necessary and dispensable elements for building smarter machines.

Acknowledgments and Disclosure of Funding

This work was supported by a Sofja Kovalevskaja Award from the Alexander von Humboldt Foundation. We acknowledge the support from the BMBF through the Tübingen AI Center (FKZ: 01IS18039A and 01IS18039B). AL, GM, and BS are members of the Machine Learning Cluster of Excellence, EXC number 2064/1 – Project number 39072764.

References

- [1] Mara Almog and Alon Korngreen. Is realistic neuronal modeling realistic? *Journal of neurophysiology*, 116(5):2180–2209, 2016.
- [2] Jaan Aru, Mototaka Suzuki, and Matthew E Larkum. Cellular mechanisms of conscious processing. *Trends in Cognitive Sciences*, 24(10):814–825, 2020.
- [3] Guillaume Bellec, Darjan Salaj, Anand Subramoney, Robert Legenstein, and Wolfgang Maass. Long short-term memory and learning-to-learn in networks of spiking neurons. *Advances in neural information processing systems*, 31, 2018.
- [4] Guillaume Bellec, Franz Scherr, Anand Subramoney, Elias Hajek, Darjan Salaj, Robert Legenstein, and Wolfgang Maass. A solution to the learning dilemma for recurrent networks of spiking neurons. *Nature Communications*, 11(1):3625, December 2020. ISSN 2041-1723. doi: 10.1038/s41467-020-17236-y. URL <http://www.nature.com/articles/s41467-020-17236-y>.
- [5] David Beniaguev, Idan Segev, and Michael London. Single cortical neurons as deep artificial neural networks. *Neuron*, 109(17):2727–2739, 2021.
- [6] Brendan A Bicknell and Michael Häusser. A synaptic learning rule for exploiting nonlinear dendritic computation. *Neuron*, 109(24):4001–4017, 2021.
- [7] Romain Brette and Wulfram Gerstner. Adaptive exponential integrate-and-fire model as an effective description of neuronal activity. *Journal of neurophysiology*, 94(5):3637–3642, 2005.
- [8] Anthony N Burkitt. A review of the integrate-and-fire neuron model: I. homogeneous synaptic input. *Biological cybernetics*, 95:1–19, 2006.
- [9] Jessica F Cantlon and Elizabeth M Brannon. Basic Math in Monkeys and College Students. *PLoS Biology*, 5(12):e328, December 2007. ISSN 1545-7885. doi: 10.1371/journal.pbio.0050328. URL <https://dx.plos.org/10.1371/journal.pbio.0050328>.
- [10] Sean E Cavanagh, Laurence T Hunt, and Steven W Kennerley. A diversity of intrinsic timescales underlie neural computations. *Frontiers in Neural Circuits*, 14:615626, 2020.
- [11] Spyridon Chavlis and Panayiota Poirazi. Drawing inspiration from biological dendrites to empower artificial neural networks. *Current opinion in neurobiology*, 70:1–10, 2021.
- [12] Kyunghyun Cho, Bart Van Merriënboer, Caglar Gulcehre, Dzmitry Bahdanau, Fethi Bougares, Holger Schwenk, and Yoshua Bengio. Learning phrase representations using rnn encoder-decoder for statistical machine translation. *arXiv preprint arXiv:1406.1078*, 2014.
- [13] Benjamin Cramer, David Stöckel, Markus Kreft, Michael Wibral, Johannes Schemmel, Karlheinz Meier, and Viola Priesemann. Control of criticality and computation in spiking neuromorphic networks with plasticity. *Nature communications*, 11(1):2853, 2020.
- [14] Benjamin Cramer, Yannik Stradmann, Johannes Schemmel, and Friedemann Zenke. The heidelberg spiking data sets for the systematic evaluation of spiking neural networks. *IEEE Transactions on Neural Networks and Learning Systems*, 2020.

- [15] Peter Dayan and Laurence F Abbott. *Theoretical neuroscience: computational and mathematical modeling of neural systems*. MIT press, 2005.
- [16] Richard Gao, Ruud L van den Brink, Thomas Pfeffer, and Bradley Voytek. Neuronal timescales are functionally dynamic and shaped by cortical microarchitecture. *Elife*, 9:e61277, 2020.
- [17] Sonia Gasparini and Jeffrey C Magee. State-dependent dendritic computation in hippocampal ca1 pyramidal neurons. *Journal of Neuroscience*, 26(7):2088–2100, 2006.
- [18] Wulfram Gerstner and Werner M Kistler. *Spiking neuron models: Single neurons, populations, plasticity*. Cambridge university press, 2002.
- [19] Wulfram Gerstner, Werner M Kistler, Richard Naud, and Liam Paninski. *Neuronal dynamics: From single neurons to networks and models of cognition*. Cambridge University Press, 2014.
- [20] Albert Gidon, Timothy Adam Zolnik, Pawel Fidzinski, Felix Bolduan, Athanasia Papoutsi, Panayiota Poirazi, Martin Holtkamp, Imre Vida, and Matthew Evan Larkum. Dendritic action potentials and computation in human layer 2/3 cortical neurons. *Science*, 367(6473):83–87, 2020.
- [21] Julijana Gjorgjieva, Guillaume Drion, and Eve Marder. Computational implications of biophysical diversity and multiple timescales in neurons and synapses for circuit performance. *Current opinion in neurobiology*, 37:44–52, 2016.
- [22] André Grüning and Sander M Bohte. Spiking neural networks: Principles and challenges. In *ESANN*. Bruges, 2014.
- [23] Albert Gu, Karan Goel, and Christopher Re. Efficiently modeling long sequences with structured state spaces. In *International Conference on Learning Representations*.
- [24] Robert Gütiğ and Haim Sompolinsky. The tempotron: a neuron that learns spike timing–based decisions. *Nature neuroscience*, 9(3):420–428, 2006.
- [25] Jeff Hawkins and Subutai Ahmad. Why neurons have thousands of synapses, a theory of sequence memory in neocortex. *Frontiers in neural circuits*, page 23, 2016.
- [26] Etay Hay, Sean Hill, Felix Schürmann, Henry Markram, and Idan Segev. Models of neocortical layer 5b pyramidal cells capturing a wide range of dendritic and perisomatic active properties. *PLoS computational biology*, 7(7):e1002107, 2011.
- [27] Andreas VM Herz, Tim Gollisch, Christian K Machens, and Dieter Jaeger. Modeling single-neuron dynamics and computations: a balance of detail and abstraction. *science*, 314(5796): 80–85, 2006.
- [28] Sepp Hochreiter and Jürgen Schmidhuber. Long short-term memory. *Neural computation*, 9(8): 1735–1780, 1997.
- [29] Shiri Hodassman, Roni Vardi, Yael Tugendhaft, Amir Goldental, and Ido Kanter. Efficient dendritic learning as an alternative to synaptic plasticity hypothesis. *Scientific Reports*, 12(1): 6571, 2022.
- [30] Alan L Hodgkin and Andrew F Huxley. A quantitative description of membrane current and its application to conduction and excitation in nerve. *The Journal of physiology*, 117(4):500, 1952.
- [31] Eugene M Izhikevich. Which model to use for cortical spiking neurons? *IEEE transactions on neural networks*, 15(5):1063–1070, 2004.
- [32] Monika P Jadi, Bardia F Behabadi, Alon Poleg-Polsky, Jackie Schiller, and Bartlett W Mel. An augmented two-layer model captures nonlinear analog spatial integration effects in pyramidal neuron dendrites. *Proceedings of the IEEE*, 102(5):782–798, 2014.
- [33] Herbert Jaeger. Tutorial on training recurrent neural networks, covering bppt, rtrl, ekf and the "echo state network" approach. ., 2002.

- [34] Renaud Jolivet, Felix Schürmann, Thomas K Berger, Richard Naud, Wulfram Gerstner, and Arnd Roth. The quantitative single-neuron modeling competition. *Biological cybernetics*, 99(4):417–426, 2008.
- [35] Ilenna Simone Jones and Konrad Paul Kording. Might a single neuron solve interesting machine learning problems through successive computations on its dendritic tree? *Neural Computation*, 33(6):1554–1571, 2021.
- [36] Ilenna Simone Jones and Konrad Paul Kording. Do biological constraints impair dendritic computation? *Neuroscience*, 489:262–274, 2022.
- [37] Eric R Kandel, James H Schwartz, Thomas M Jessell, Steven Siegelbaum, A James Hudspeth, Sarah Mack, et al. *Principles of neural science*, volume 4. McGraw-hill New York, 2000.
- [38] Ryota Kobayashi, Yasuhiro Tsubo, and Shigeru Shinomoto. Made-to-order spiking neuron model equipped with a multi-timescale adaptive threshold. *Frontiers in computational neuroscience*, page 9, 2009.
- [39] Christof Koch. Computation and the single neuron. *Nature*, 385(6613):207–210, 1997.
- [40] Christof Koch and Idan Segev. The role of single neurons in information processing. *Nature neuroscience*, 3(11):1171–1177, 2000.
- [41] Peter König, Andreas K Engel, and Wolf Singer. Integrator or coincidence detector? the role of the cortical neuron revisited. *Trends in neurosciences*, 19(4):130–137, 1996.
- [42] Alex Krizhevsky, Geoffrey Hinton, et al. Learning multiple layers of features from tiny images. 2009.
- [43] Aditya Kusupati, Manish Singh, Kush Bhatia, Ashish Kumar, Prateek Jain, and Manik Varma. Fastgrnn: A fast, accurate, stable and tiny kilobyte sized gated recurrent neural network. *Advances in neural information processing systems*, 31, 2018.
- [44] Esther F. Kutter, Jan Bostroem, Christian E. Elger, Florian Mormann, and Andreas Nieder. Single Neurons in the Human Brain Encode Numbers. *Neuron*, 100(3):753–761.e4, November 2018. ISSN 08966273. doi: 10.1016/j.neuron.2018.08.036. URL <https://linkinghub.elsevier.com/retrieve/pii/S0896627318307414>.
- [45] Esther F. Kutter, Jan Boström, Christian E. Elger, Andreas Nieder, and Florian Mormann. Neuronal codes for arithmetic rule processing in the human brain. *Current Biology*, 32(6):1275–1284.e4, March 2022. ISSN 09609822. doi: 10.1016/j.cub.2022.01.054. URL <https://linkinghub.elsevier.com/retrieve/pii/S0960982222001166>.
- [46] Mathieu Lafourcade, Marie-Sophie H van der Goes, Dimitra Vardalaki, Norma J Brown, Jakob Voigts, Dae Hee Yun, Minyoung E Kim, Taeyun Ku, and Mark T Harnett. Differential dendritic integration of long-range inputs in association cortex via subcellular changes in synaptic ampa-to-nmda receptor ratio. *Neuron*, 2022.
- [47] Matthew Larkum. Are dendrites conceptually useful? *Neuroscience*, 2022.
- [48] Drew Linsley, Junkyung Kim, Vijay Veerabadran, Charles Windolf, and Thomas Serre. Learning long-range spatial dependencies with horizontal gated recurrent units. *Advances in neural information processing systems*, 31, 2018.
- [49] Xuezhe Ma, Chunting Zhou, Xiang Kong, Junxian He, Liangke Gui, Graham Neubig, Jonathan May, and Luke Zettlemoyer. Mega: Moving average equipped gated attention. In *The Eleventh International Conference on Learning Representations*, 2023. URL <https://openreview.net/forum?id=qNLe3iq2E1>.
- [50] Wolfgang Maass. Networks of spiking neurons: the third generation of neural network models. *Neural networks*, 10(9):1659–1671, 1997.
- [51] Shivangi Mahto, Vy Ai Vo, Javier S. Turek, and Alexander Huth. Multi-timescale representation learning in {lstm} language models. In *International Conference on Learning Representations*, 2021. URL <https://openreview.net/forum?id=9ITXiTrAoT>.

- [52] Guy Major, Matthew E Larkum, and Jackie Schiller. Active properties of neocortical pyramidal neuron dendrites. *Annual review of neuroscience*, 36:1–24, 2013.
- [53] Joseph Marino. Predictive coding, variational autoencoders, and biological connections. *Neural Computation*, 34(1):1–44, 2021.
- [54] Toviah Moldwin and Idan Segev. Perceptron learning and classification in a modeled cortical pyramidal cell. *Frontiers in computational neuroscience*, 14:33, 2020.
- [55] Michael C Mozer. Induction of multiscale temporal structure. *Advances in neural information processing systems*, 4, 1991.
- [56] John D. Murray, Alberto Bernacchia, David J. Freedman, Ranulfo Romo, Jonathan D. Wallis, Xinying Cai, Camillo Padoa-Schioppa, Tatiana Pasternak, Hyojung Seo, Daeyeol Lee, and Xiao-Jing Wang. A hierarchy of intrinsic timescales across primate cortex. *Nature Neuroscience*, 17(12):1661–1663, December 2014. ISSN 1546-1726. doi: 10.1038/nn.3862. URL <https://www.nature.com/articles/nn.3862>.
- [57] Panayiota Poirazi and Athanasia Papoutsis. Illuminating dendritic function with computational models. *Nature Reviews Neuroscience*, 21(6):303–321, 2020.
- [58] Panayiota Poirazi, Terrence Brannon, and Bartlett W Mel. Pyramidal neuron as two-layer neural network. *Neuron*, 37(6):989–999, 2003.
- [59] R Angus Silver. Neuronal arithmetic. *Nature Reviews Neuroscience*, 11(7):474–489, 2010.
- [60] Jimmy T.H. Smith, Andrew Warrington, and Scott Linderman. Simplified state space layers for sequence modeling. In *The Eleventh International Conference on Learning Representations*, 2023. URL <https://openreview.net/forum?id=Ai8Hw3AXqks>.
- [61] Greg J Stuart and Nelson Spruston. Dendritic integration: 60 years of progress. *Nature neuroscience*, 18(12):1713–1721, 2015.
- [62] Corentin Tallec and Yann Ollivier. Can recurrent neural networks warp time? In *International Conference on Learning Representations*, 2018.
- [63] Yuanhong Tang, Xingyu Zhang, Lingling An, Zhaofei Yu, and Jian K Liu. Diverse role of nmda receptors for dendritic integration of neural dynamics. *PLOS Computational Biology*, 19(4): e1011019, 2023.
- [64] Yi Tay, Mostafa Dehghani, Samira Abnar, Yikang Shen, Dara Bahri, Philip Pham, Jinfeng Rao, Liu Yang, Sebastian Ruder, and Donald Metzler. Long range arena : A benchmark for efficient transformers. In *International Conference on Learning Representations*, 2021. URL <https://openreview.net/forum?id=qVyeW-grC2k>.
- [65] Alexandra Tzivilivaki, George Kastellakis, and Panayiota Poirazi. Challenging the point neuron dogma: Fs basket cells as 2-stage nonlinear integrators. *Nature communications*, 10(1):3664, 2019.
- [66] Balázs B Ujfalussy, Judit K Makara, Máté Lengyel, and Tiago Branco. Global and multiplexed dendritic computations under in vivo-like conditions. *Neuron*, 100(3):579–592, 2018.
- [67] Jos Van Der Westhuizen and Joan Lasenby. The unreasonable effectiveness of the forget gate. *arXiv preprint arXiv:1804.04849*, 2018.
- [68] Ashish Vaswani, Noam Shazeer, Niki Parmar, Jakob Uszkoreit, Llion Jones, Aidan N Gomez, Łukasz Kaiser, and Illia Polosukhin. Attention is all you need. *Advances in neural information processing systems*, 30, 2017.
- [69] Qu Yang, Jibin Wu, and Haizhou Li. Rethinking benchmarks for neuromorphic learning algorithms. In *2021 International Joint Conference on Neural Networks (IJCNN)*, pages 1–8. IEEE, 2021.

- [70] Friedemann Zenke and Tim P Vogels. The remarkable robustness of surrogate gradient learning for instilling complex function in spiking neural networks. *Neural Computation*, 33(4):899–925, 2021.
- [71] Roxana Zeraati, Yan-Liang Shi, Nicholas A Steinmetz, Marc A Gieselmann, Alexander Thiele, Tirin Moore, Anna Levina, and Tatiana A Engel. Intrinsic timescales in the visual cortex change with selective attention and reflect spatial connectivity. *Nature Communications*, 14(1):1858, 2023.

Appendix

A Implementation Details

All computations were performed using Python 3.9, and the following libraries were instrumental in our implementation: jax 0.3.14 (coupled with jaxlib 0.3.10 as a GPU back-end) for auto-grad and auto-vectorization; equinox 0.8.0, a jax-based neural network library; optax 0.1.3, a jax-based optimizer library; and pytorch 1.12.1 for data-loading. The code used for our experiments will be accessible at the public repository upon publication. To maintain anonymity, the essential excerpts of the code are presented in Section E.

Table S1: The default ELM neuron parameters and recommendations.

Hyper-Parameter	NeuronIO	Tuning Recommendation
s_0	0	/
w_s	0.5	/
w_s (bounds)	> 0	≥ 0
τ_s	5ms	greater for long and sparse data
m_0	0	/
d_m	20	between 10 – 250
τ_m (init technique)	equally spaced	evenly spaced on logarithmic scale
τ_m (init range)	1ms,100ms	1ms to sample length in ms
τ_m (bounds)	0ms,500ms	same as init range or larger
MLP w_p (nonlinear)	ReLU	/
MLP w_p (bias)	True	/
MLP w_p (init technique)	Kaiming Uniform	/
l_{mlp}	1	/
d_{mlp}	$2 * d_m$	$2 * d_m$
λ	10	between 1 – 10
w_y (bias)	True	/
w_y (init technique)	Kaiming Uniform	/
d_{tree}	45	receive all input 2-5 times over
d_{brch}	100	$2 * d_{tree}$

Recommended default and tuning parameters: On a novel dataset, we recommend starting with a smaller d_m around 100, and small λ around 3, as increasing both simultaneously may lead to increased training instability. Potential future work could explore setting λ automatically based on d_m , or learning it directly. The timescales τ_m should generally be derived from the dataset length and the suspected timescales of the temporal dependencies within the data. Increasing τ_s may help to enhance learning speed in some cases. When using the (branch) ELM it is important to sufficiently over-sample the input (more synapses than input) as significant expressivity stems from w_s doing the selection. Additional recommendations are summarized in Table S1.

B Datasets and Training Details

General training setup: For each task and dataset, the training dataset was deterministically split to create a consistent validation dataset, which was used for model selection during training and hyperparameter tuning. By default all models were trained using Backpropagation Through Time (BPTT) with a batch size of 8 and the Adam optimizer, employing a learning rate of $5e^{-4}$ and a cosine-decay schedule across the entire training duration. All experiments were run on a single A100-40GB or A100-80GB and ran less than 24h, Pathfinder-X being the notable exception.

NeuronIO Dataset: For training and evaluation the dataset was pre-processed in accordance with [5], by capping somatic membrane voltage at -55mV and subtracting a bias of -67.7mV. Additionally, the somatic membrane voltage was scaled by 1/10 for training. Training samples were 500ms long with a 1ms bin size and Δt . The ELM neuron used the default parameters from Table S1. Models

were trained for 30 epochs of 11,400 batches per epoch using Binary Cross Entropy (BCE) for spike prediction and Mean Squared Error (MSE) for somatic voltage prediction, with equal weighting. Loss was calculated after a 150ms burn-in period. The mean and standard deviation over three runs is reported, with Root Means Squared Error (RMSE) and Area Under the Receiver Operator Curve (AUC) for voltage and spike prediction, respectively.

Spiking Heidelberg Digits (Adding) Datasets: The digits were preprocessed by cutting them to a uniform length of one second and binning the spikes using various bin sizes, the default being 10ms. The models were trained using the Adamax optimizer with a learning rate of $5e^{-3}$ for 70 epochs, for 814 and 2000 batches per epoch for SHD and SHD-Adding respectively, with Δt set to the bin size, and dropout probability set to 0.5. The ELM used $\lambda = 5$, $d_m = 100$ and τ_m initialized evenly spaced between 1ms and 150ms with bounds of 0ms to 1000ms, and the LSTM used a hidden size of 250 and additional recurrent dropout of 0.3, while the SNN used a learning rate of $2e^{-3}$ no dropout but a $l1$ regularization on the spikes of 0.01. Models were trained using the Cross-Entropy (CE) loss on the last float output of the respective model, and the performance was reported as prediction Accuracy, with mean and standard deviation calculated over five runs (chance performance being 1/19).

Long Sequence Modeling Datasets: The images were preprocessed by binning the 256 greyscale values into 16 values, and 32 different values for Pathfinder-X. The models were trained for 300 epochs with a batch size of 384, and batch size of 768 for Pathfinder-X. All trained using Cross-Entropy (CE) loss on the last output of the model, and the performance is reported as prediction Accuracy. The mean over three runs is reported for all experiments.

Table S2: The ELM neuron configuration

Dataset	Data Bins	Batch Size	LR	d_m	λ	Timescales
CIFAR-10	16	384	$1e^{-3}$	150	3	logspace: $1 - 10^3$
Pathfinder	16	384	$3e^{-4}$	150	3	logspace: $1 - 10^3$
Pathfinder-X	32	768	$2e^{-4}$	150	5	logspace: $1 - 10^4$

The ELM memory timescale bounds were matched to the initialization range. On the Pathfinder dataset an additional input dropout of 0.2 was applied, however using $lr = 2e^{-4}$ and no dropout still achieves 71.61% accuracy. Furthermore, the ELM used a synapse tau of 150ms on the Pathfinder-X dataset, which we observed to increase the learning speed.

Table S3: The Chrono-LSTM configuration

Dataset	Data Bins	Batch Size	LR	Hidden Size	Timescales
CIFAR-10	16	384	$1e^{-3}$	150	uniform: $1 - 2 * 10^3$
Pathfinder	16	384	$1e^{-3}$	150	uniform: $1 - 2 * 10^3$
Pathfinder-X	32	768	$1e^{-3}$	70	uniform: $1 - 2 * 10^4$

Alternative configurations for the Chrono-LSTM model, including learning rates of $2e^{-4}$, $5e^{-4}$, and $7e^{-4}$, as well as a hidden size of 150 with half the batch size (reaching the 80GB GPU memory limit), were evaluated. For Pathfinder-X, only the reported configuration demonstrated performance exceeding chance levels, and only for one of the three trials.

C Additional Results

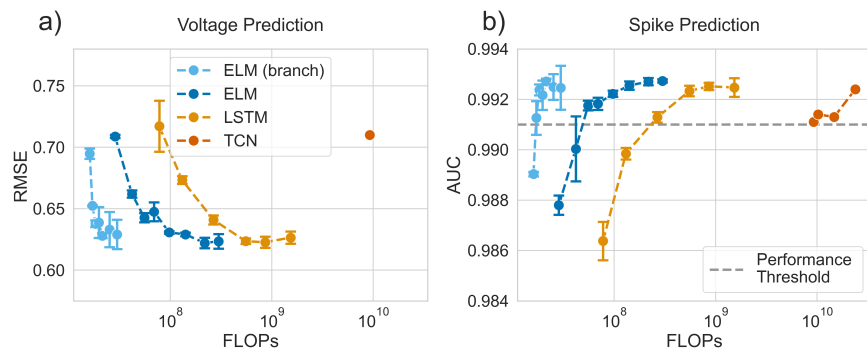


Figure S1: **The ELM neuron is a computationally efficient model of cortical neuron.** Similar figure to 2c and 2d, however, displaying FLOPs required to do inference on a single sample. **a) and b)** Voltage and spike prediction performance of the respective surrogate models. While previous works required around 10M parameters to make accurate spike predictions using a **TCN** [5], an **LSTM** baseline is able to do it with 266K, our **ELM** neuron requires merely 53K, and our **(branch) ELM** neuron only a humble 8K, simultaneously achieving much better voltage prediction performance than the **TCN**. A throughput optimized ELM neuron implementation can potentially reduce the required FLOPs even further.

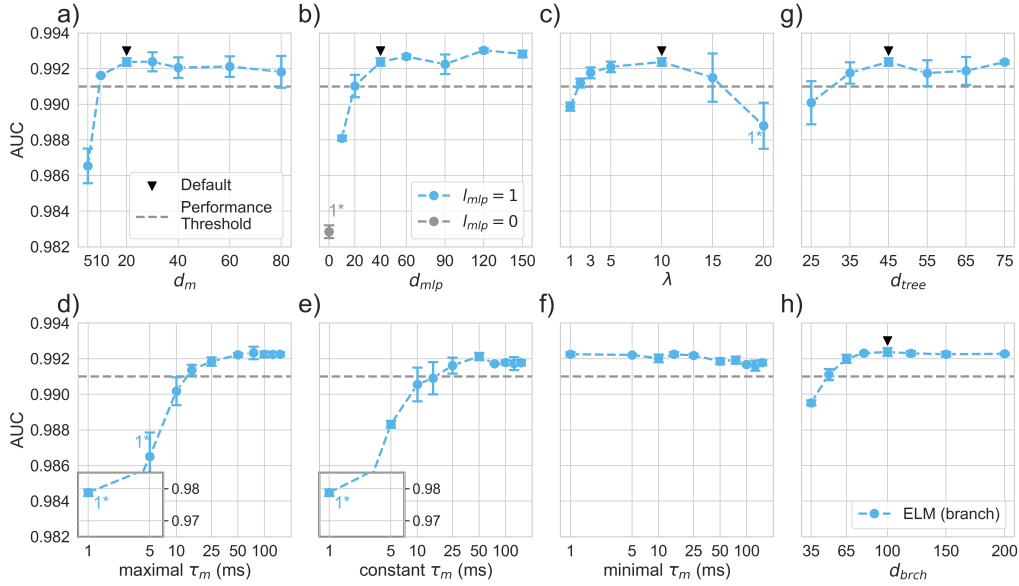


Figure S2: **The ELM neuron gives relevant neuroscientific insights.** Ablations on NeuronIO of different hyperparameters of an (branch) ELM neuron with $AUC \approx 0.992$, with default hyperparameters. The number of removed divergent runs marked with 1^* . **a)** We find above memory-like hidden states to be required for accurate predictions, much more than typical phenomenological models use [31, 15]. **b)** Highly nonlinear integration of synaptic input is required, in line with recent neuroscientific findings [61, 36, 47]. **c)** Allowing greater updates to the memory units is beneficial, however, too large ones increase training instability. **d-f)** Ablations of memory timescale (initialization and bounding) range or (constant) value, with the default range being 1ms-150ms. Timescales around 25ms-50ms seem to be the most useful (matching the typical membrane timescale in the cortex [15]); however, a lack can be partially compensated by longer timescales, even better than by the vanilla ELM. **g) and h)** Ablating the number of branches d_{tree} and number of synapses per branch d_{brch} .

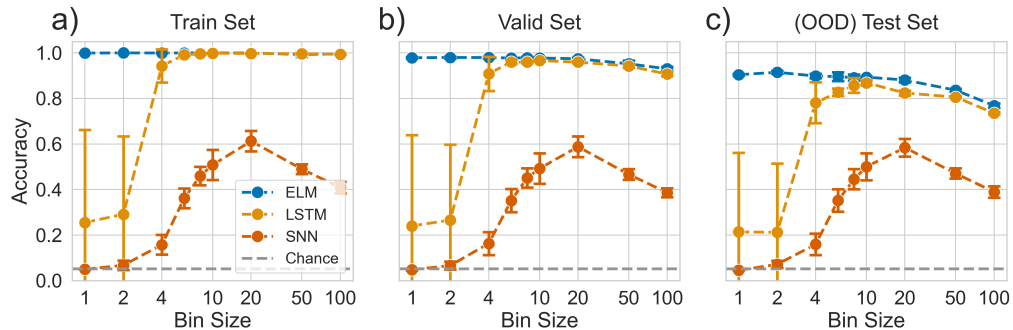


Figure S3: **The ELM neuron performs well on typical spiking datasets.** The following results are on the original Spiking Heidelberg Digits dataset [14]. **a-c)** The ELM neuron consistently outperforms a classic LSTM, especially for smaller bin sizes (meaning longer training samples), and LSTM-performance cannot be fully recovered even for larger bin sizes. Our Leaky Integrate and Fire (LIF) Spiking Neural Network (SNN), however, does manage to achieve decent performance for intermediate bin sizes around 20, in contrast to the SHD-Adding dataset (see Figure 5).

D Additional Visualizations

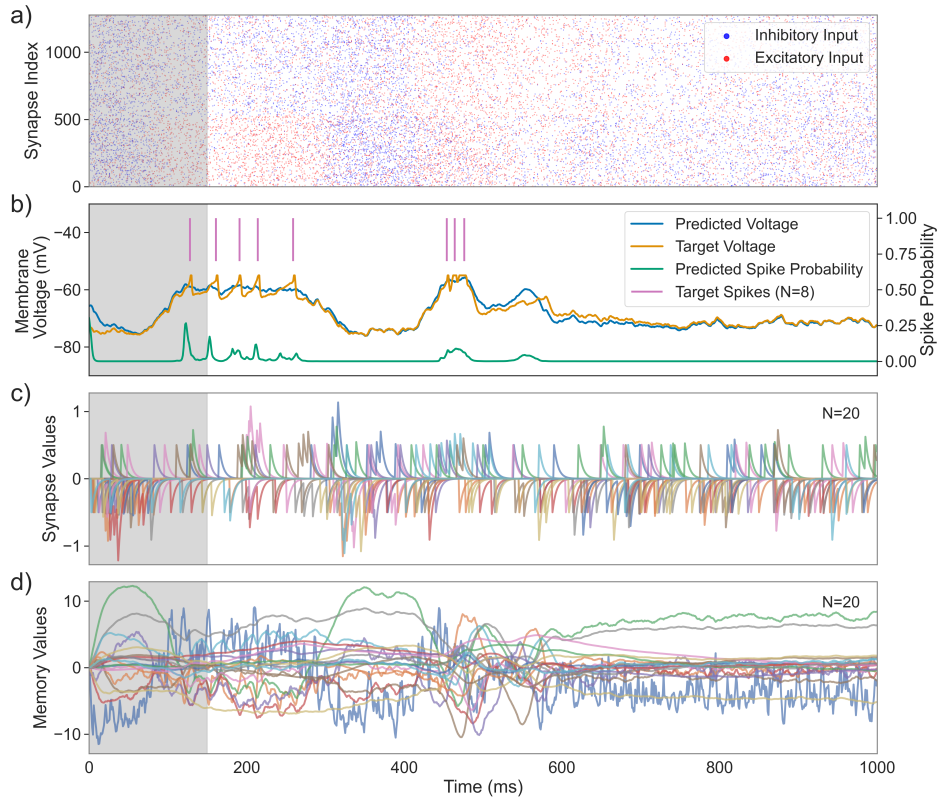


Figure S4: **Visualization of ELM neuron dynamics.** Extended visualization of Figure 2b for an ELM neuron achieving around 0.992 AUC. **a)** The synaptic input as the neuron model receives it, with excitatory input (+1) marked in red, and inhibitory input (-1) marked in blue. **b)** The ELM neurons predictions and the ground-truth targets, for a particularly challenging example. **c)** A random subset of 20 synapses are visualized. Synapses receiving negative input will be deflected downwards. **d)** All 20 memory values are visualized. Some fluctuate more rapidly than others, typically proportional to their memory timescales.

E Reduced Implementation In Pytorch

```

import math
import torch
import torch.nn as nn

# NOTE: the 1e-6 used throughout are to avoid numerical instabilities
# NOTE: the tau_m bounds are enforced using a scaled sigmoid
# NOTE: the w_s bounds are enforced using relu (originally exp)

def scaled_sigmoid(x, lower_bound, upper_bound):
    return (upper_bound - lower_bound) * torch.sigmoid(x) + lower_bound

def inverse_scaled_sigmoid(x, lower_bound, upper_bound):
    x = torch.clamp(x, lower_bound + 1e-6, upper_bound - 1e-6)
    return torch.log((x - lower_bound) / (upper_bound - x))

def custom_tanh(x):
    return torch.tanh(x * 2 / 3) * 1.7159

class MLP(nn.Module):
    """Multi-layer perceptron (MLP) model."""

    def __init__(self, input_size, hidden_size, num_output, num_layers):

```

```

super(MLP, self).__init__()
next_input_size = input_size

layers = []
for i in range(num_layers):
    layers.append(nn.Linear(next_input_size, hidden_size))
    layers.append(nn.ReLU())
    next_input_size = hidden_size

layers.append(nn.Linear(next_input_size, num_output))
self.network = nn.Sequential(*layers)

def forward(self, x):
    return self.network(x)

class ELM(nn.Module):
    """Expressive Leaky Memory (ELM) neuron model."""

    def __init__(self, num_synapse, num_output, num_memory=100,
                mlp_num_layers=1, memory_tau_min=10, memory_tau_max=1000,
                lambda_value=3.0, tau_s_value=5.0, w_s_value=0.5, delta_t=1.0,
                learn_memory_tau=False, mlp_hidden_size=None, use_num_branch=None):
        super(ELM, self).__init__()
        self.delta_t = delta_t
        self.lambda_value = lambda_value
        self.learn_memory_tau = learn_memory_tau
        self.memory_tau_min = memory_tau_min
        self.memory_tau_max = memory_tau_max

        # configuration in case of using branches
        self.use_num_branch = use_num_branch
        if use_num_branch is not None:
            assert num_synapse % use_num_branch == 0, "must_be_exactly_divisible"
            num_mlp_input = use_num_branch + num_memory
        else:
            num_mlp_input = num_synapse + num_memory

        # initialization of model parameters
        mlp_hidden_size = mlp_hidden_size if mlp_hidden_size else 2 * num_memory
        self.mlp = MLP(num_mlp_input, mlp_hidden_size, num_memory, mlp_num_layers)
        self.w_s = nn.parameter.Parameter(torch.full((num_synapse, ), w_s_value))
        self.w_y = nn.Linear(num_memory, num_output)

        # initialization of time constants and decay factors
        self.tau_s = torch.full((num_synapse, ), tau_s_value)
        self.kappa_s = torch.exp(-delta_t / torch.clamp(self.tau_s, min=1e-6))
        self._proto_tau_m = torch.logspace(
            math.log10(memory_tau_min + 1e-6),
            math.log10(memory_tau_max - 1e-6),
            num_memory,
        )
        self._proto_kappa_m = torch.exp(
            -delta_t / torch.clamp(self._proto_tau_m, min=1e-6)
        )

        # configuration in case memory tau is learnable
        if self.learn_memory_tau:
            self._proto_tau_m = inverse_scaled_sigmoid(
                self._proto_tau_m, memory_tau_min, memory_tau_max
            )
            self._proto_tau_m = nn.parameter.Parameter(self._proto_tau_m)

    @property
    def tau_m(self):
        # ensure that tau_m is always up to date
        if self.learn_memory_tau:
            return scaled_sigmoid(
                self._proto_tau_m, self.memory_tau_min, self.memory_tau_max
            )
        else:
            return self._proto_tau_m

    @property
    def kappa_m(self):
        # ensure that kappa_m is always up to date
        if self.learn_memory_tau:
            return torch.exp(-self.delta_t / torch.clamp(self.tau_m, min=1e-6))
        else:
            return self._proto_kappa_m

    def dynamics(self, x, s_prev, m_prev, kappa_m):

```

```

# compute the dynamics for a single timestep
batch_size = x.shape[0]
s_t = self.kappa_s * s_prev + torch.relu(self.w_s) * x
if self.use_num_branch is not None:
    syn_input = s_t.view(batch_size, self.use_num_branch, -1).sum(dim=-1)
else:
    syn_input = s_t
delta_m_t = custom_tanh(
    self.mlp(torch.cat([syn_input, kappa_m * m_prev], dim=-1))
)
m_t = kappa_m * m_prev + self.lambda_value * (1 - kappa_m) * delta_m_t
y_t = self.w_y(m_t)
return y_t, s_t, m_t

def forward(self, X):
# compute the recurrent dynamics for a sample
batch_size, T, num_synapse = X.shape
kappa_m = self.kappa_m
s_prev = torch.zeros(batch_size, len(self.tau_s), device=X.device)
m_prev = torch.zeros(batch_size, len(self.tau_m), device=X.device)
outputs = []
for t in range(T):
    y_t, s_prev, m_prev = self.dynamics(X[:, t], s_prev, m_prev, kappa_m)
    outputs.append(y_t)
return torch.stack(outputs, dim=-2)

```

F Results in Table Format

Table S4: The (branch) ELM on NeuronIO

Memory Units	Trainable Parameters	FLOPs	Voltage Prediction RMSE	Spike Prediction AUC
10	5.9K	16.04M	0.695 ± 0.004	0.989 ± 0.0001
15	6.9K	17.06M	0.652 ± 0.0	0.9913 ± 0.0007
20	8.1K	18.27M	0.638 ± 0.003	0.9924 ± 0.0002
25	9.5K	19.69M	0.639 ± 0.013	0.9922 ± 0.0006
30	11.1K	21.3M	0.628 ± 0.002	0.9927 ± 0.0001
40	14.9K	25.13M	0.633 ± 0.014	0.9925 ± 0.0005
50	19.5K	29.76M	0.629 ± 0.012	0.9925 ± 0.0009

Table S5: The ELM on NeuronIO

Memory Units	Trainable Parameters	FLOPs	Voltage Prediction RMSE	Spike Prediction AUC
10	26.06K	28.49M	0.709 ± 0.001	0.9878 ± 0.0004
15	39.39K	41.84M	0.662 ± 0.003	0.99 ± 0.0013
20	52.92K	55.38M	0.643 ± 0.004	0.9918 ± 0.0002
25	66.65K	69.13M	0.648 ± 0.008	0.9918 ± 0.0002
35	94.71K	97.22M	0.631 ± 0.001	0.9922 ± 0.0001
50	138.3K	140.85M	0.629 ± 0.002	0.9925 ± 0.0002
75	214.95K	217.58M	0.622 ± 0.004	0.9927 ± 0.0001
100	296.6K	299.3M	0.623 ± 0.006	0.9927 ± 0.0001

Table S6: The LSTM on NeuronIO

Hidden Size	Trainable Parameters	FLOPs	Voltage Prediction RMSE	Spike Prediction AUC
15	77.67K	77.77M	0.717 ± 0.021	0.9864 ± 0.0008
25	130.45K	130.61M	0.673 ± 0.003	0.9898 ± 0.0002
50	265.9K	266.23M	0.641 ± 0.004	0.9913 ± 0.0002
100	551.8K	552.45M	0.624 ± 0.002	0.9923 ± 0.0002
150	857.7K	858.68M	0.623 ± 0.005	0.9925 ± 0.0001
250	1529.5K	1531.13M	0.626 ± 0.005	0.9925 ± 0.0004

Table S7: SHD Results

Model	Bin Size	Train Accuracy	Valid Accuracy	Test Accuracy
ELM	1	1.0 ± 0.0	0.98 ± 0.0	0.9 ± 0.0
	2	1.0 ± 0.0	0.98 ± 0.0	0.91 ± 0.01
	4	1.0 ± 0.0	0.98 ± 0.0	0.9 ± 0.01
	6	1.0 ± 0.0	0.98 ± 0.0	0.9 ± 0.02
	8	1.0 ± 0.0	0.98 ± 0.0	0.89 ± 0.01
	10	1.0 ± 0.0	0.98 ± 0.0	0.89 ± 0.0
	20	1.0 ± 0.0	0.97 ± 0.0	0.88 ± 0.01
	50	0.99 ± 0.01	0.95 ± 0.01	0.84 ± 0.01
	100	1.0 ± 0.0	0.93 ± 0.01	0.77 ± 0.01
LSTM	1	0.26 ± 0.41	0.24 ± 0.4	0.21 ± 0.35
	2	0.29 ± 0.34	0.27 ± 0.33	0.21 ± 0.3
	4	0.94 ± 0.07	0.91 ± 0.07	0.78 ± 0.09
	6	0.99 ± 0.0	0.96 ± 0.01	0.83 ± 0.02
	8	1.0 ± 0.0	0.96 ± 0.0	0.86 ± 0.03
	10	1.0 ± 0.0	0.97 ± 0.0	0.87 ± 0.01
	20	1.0 ± 0.0	0.96 ± 0.0	0.82 ± 0.01
	50	1.0 ± 0.0	0.94 ± 0.01	0.81 ± 0.0
	100	0.99 ± 0.0	0.91 ± 0.01	0.74 ± 0.0
SNN	1	0.05 ± 0.0	0.05 ± 0.0	0.05 ± 0.0
	2	0.07 ± 0.02	0.07 ± 0.02	0.07 ± 0.02
	4	0.16 ± 0.04	0.16 ± 0.05	0.16 ± 0.05
	6	0.36 ± 0.04	0.35 ± 0.05	0.35 ± 0.05
	8	0.46 ± 0.04	0.45 ± 0.04	0.45 ± 0.04
	10	0.51 ± 0.07	0.49 ± 0.07	0.5 ± 0.06
	20	0.61 ± 0.04	0.59 ± 0.05	0.58 ± 0.04
	50	0.49 ± 0.02	0.47 ± 0.02	0.47 ± 0.02
	100	0.41 ± 0.03	0.39 ± 0.02	0.39 ± 0.03

Table S8: SHD-Adding Results

Model	Bin Size	Train Accuracy	Valid Accuracy	Test Accuracy
ELM	1	1.0 ± 0.0	0.96 ± 0.01	0.82 ± 0.01
	2	1.0 ± 0.0	0.96 ± 0.0	0.82 ± 0.01
	4	0.98 ± 0.03	0.93 ± 0.03	0.81 ± 0.03
	6	0.95 ± 0.05	0.89 ± 0.05	0.76 ± 0.07
	8	0.94 ± 0.09	0.88 ± 0.09	0.76 ± 0.08
	10	0.98 ± 0.04	0.93 ± 0.04	0.8 ± 0.03
	20	0.99 ± 0.0	0.94 ± 0.01	0.79 ± 0.02
	50	0.99 ± 0.0	0.92 ± 0.01	0.75 ± 0.01
	100	0.98 ± 0.0	0.86 ± 0.01	0.66 ± 0.02
LSTM	1	0.1 ± 0.0	0.1 ± 0.0	0.1 ± 0.01
	2	0.1 ± 0.0	0.1 ± 0.0	0.1 ± 0.0
	4	0.1 ± 0.0	0.1 ± 0.0	0.1 ± 0.0
	6	0.1 ± 0.0	0.1 ± 0.0	0.1 ± 0.0
	8	0.11 ± 0.02	0.11 ± 0.02	0.1 ± 0.01
	10	0.21 ± 0.08	0.19 ± 0.07	0.15 ± 0.05
	20	0.83 ± 0.37	0.75 ± 0.33	0.6 ± 0.26
	50	0.99 ± 0.0	0.87 ± 0.01	0.67 ± 0.02
	100	0.98 ± 0.0	0.75 ± 0.01	0.55 ± 0.01
SNN	10	0.09 ± 0.01	0.09 ± 0.01	0.08 ± 0.01
	20	0.08 ± 0.01	0.08 ± 0.01	0.08 ± 0.01
	50	0.1 ± 0.01	0.1 ± 0.01	0.1 ± 0.0
	100	0.09 ± 0.0	0.09 ± 0.0	0.09 ± 0.0